

Chapter 3

Efforts Toward a High Throughput Assay for Gating of the Mechanosensitive Channel of Large Conductance

Abstract

The bacterial mechanosensitive channel of large conductance (MscL) is an ideal starting point for understanding the molecular basis of mechanosensation. However, current methods for the characterization of its mutants, patch clamp and bacterial growth analysis, are difficult and time consuming, so a higher throughput method for screening mutants is desired. We have attempted to develop a fluorescence assay for detecting MscL activity in synthetic vesicles. The assay involved the separation of two solutions—one inside and one outside the vesicles—that are separately nonfluorescent but fluorescent when mixed. It was hoped that MscL activity due to downshock of the vesicles would bring about mixing of the solutions, producing fluorescence. The development of the assay required the optimization of several variables: the method for producing a uniform vesicle population containing MscL, the fluorescence system, and the lipid and protein composition of the vesicles. However, no MscL activity was ever detected even after optimization, so the assay was not fully developed. The probable cause of the failure was the inability of current techniques to produce a sufficiently uniform vesicle population.

INTRODUCTION

The Mechanosensitive Channel of Large Conductance

The ability to detect and respond to pressure stimuli is essential for an organism to survive. This process, called mechanosensation, is fundamentally involved in many sensory events in all forms of life, such as touch, hearing, and balance in animals, gravitropism and turgor pressure regulation in plants, and osmotic regulation for many cell types, particularly in bacteria and archaea [1–3]. In all of these processes, transmembrane proteins called mechanosensitive ion channels play a key role [4]. These proteins transduce a mechanical signal such as movement or an increased membrane tension into a conformational change, resulting in the formation of an ion-permeable channel through the membrane. Mechanosensitive channels have been discovered in more than thirty cell types in many kinds of organisms.

Mechanosensitive channels play an especially crucial role in osmotic pressure regulation in bacteria. Because bacteria are single-celled organisms unable to traverse large distances, sudden inundation is a threat to their survival. A rapid decrease in the external osmotic pressure, called osmotic downshock, results in a great influx of water through their cellular membranes, causing swelling. Without appropriate defenses, cell death due to lysis would occur with even a mild downshock.

Three bacterial channels—the mechanosensitive channels of large, small, and “mini” conductance (MscL, MscS, and MscM, respectively)—are thought to function as “release valves” to protect the cell during osmotic downshock (fig. 3.1) [5, 6]. When the cellular swelling during downshock increases the tension in the membrane, the channels respond to the accompanying deformation of the lipid bilayer by opening pores in the

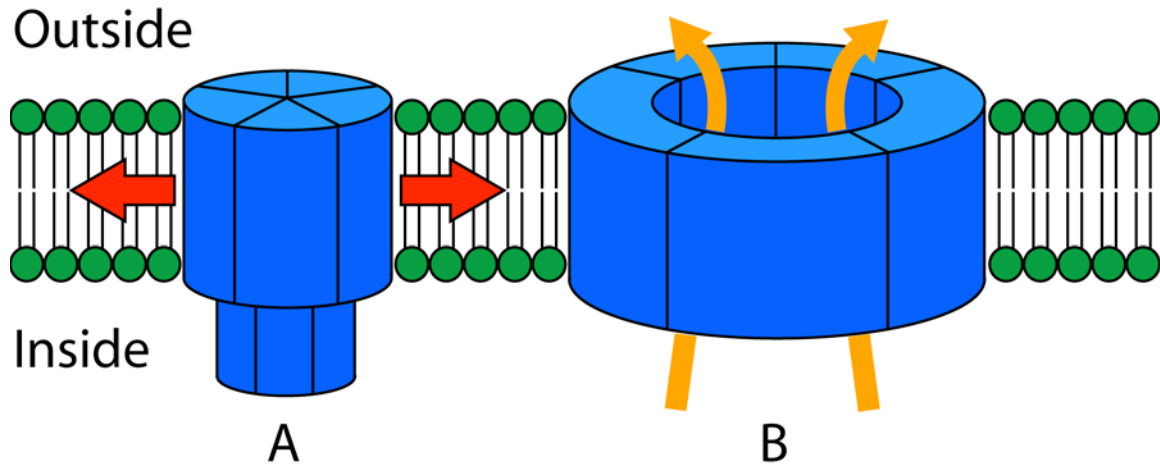


Fig. 3.1. Schematic of the mechanosensation of MscL. Under resting conditions, MscL is in the closed state (A). Osmotic downshock increases the tension in the membrane (red arrows), resulting in a transition to the open state (B). The wide pore of the open state allows the release of intracellular osmolytes (orange arrows), hopefully equilibrating the internal and external osmotic pressures before cell lysis. The outside and inside of the bacterium are noted.

membrane. The cell, instead of swelling to the point of lysis, uses the channels for a somewhat controlled equilibration of the internal and external solutions. The equilibration reduces the osmotic pressure difference, thereby preserving the bacterium.

The three channels differ in their sensitivities to membrane tension. MscM opens at lower tensions than MscS, and MscL requires the largest tension of all for gating (~ 10 dyn/cm) [5, 7]. This pattern suggests that these channels form different lines of defense, with MscL serving as bacteria's last resort for osmoprotection. MscL is activated only if the less severe activities of MscM and MscS fail to rescue the swelling cell [5].

E. coli MscL was the first mechanosensitive channel to be cloned [8].

Homologues have since been found in over 30 species of bacteria [9], and many of these have been cloned as well. Functional characterization of *E. coli* MscL has shown that it opens a large pore. Patch clamping experiments have determined that gating results in a

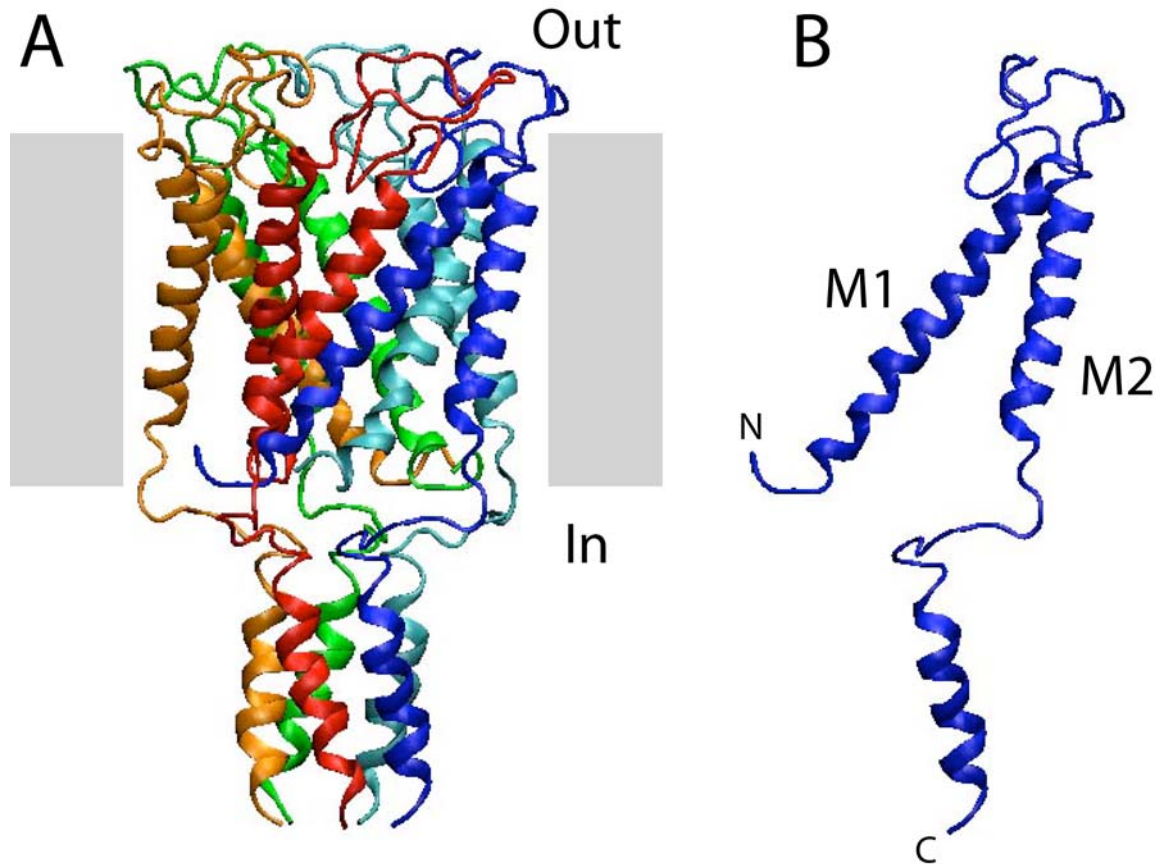


Fig. 3.2. The MscL crystal structure. MscL consists of a homopentamer (A) of identical subunits, one of which is shown (B) with the TM helices M1 and M2 and the N- and C-termini marked. The gray rectangles in A note the probable location of the membrane. The inside and outside of the cell are also indicated. The protein images were prepared with VMD.

highly conductive (~ 3.0 nS), nonspecific channel [10]. In addition, biochemical studies have shown that both ions and small molecules such as ATP can pass through MscL [10]. It is possible that MscL even allows the release of the small proteins EF-Tu, DnaK, and thioredoxin [11, 12], although this claim has been disputed [13]. The permeability data indicate that the pore is 36–42 Å in diameter, extremely large among ion channels [14].

The crystal structure of the closed state of the *M. tuberculosis* homologue of MscL shows that the functional unit is a homopentamer (fig. 3.2A) [15]. Each subunit has two transmembrane (TM) domains M1 and M2 (fig. 3.2B), which are well conserved

across species. Both the N- and C-termini are cytoplasmic [16]. The gate of the channel is formed by the N-terminal part of M1, and the M2 helices form a shell on the periphery of the protein adjacent to the lipid. Each subunit of *E. coli* MscL contains 136 residues [8], the last ~50 of which extend into the cytoplasm and form a pentameric helical bundle [15]. Deletion experiments have shown that the cytoplasmic portion is not necessary for forming a functional channel [17], and its function is still unclear.

Because mechanosensitive channels are important in a wide variety of critical processes, it is of great interest to understand the molecular basis for their function, including their mechanisms for sensing mechanical signals and gating, which are still poorly understood. MscL is invaluable as a model system for the more complicated channels found in higher organisms. Because of its simplicity, understanding MscL and its mutants is an ideal starting point for the study of the principles of mechanosensation. An important step in achieving this goal is the development of an assay to quickly and easily screen MscL mutants, identifying the most promising for more detailed study.

Current Techniques for Studying MscL

Presently, two general techniques—patch-clamp analysis and bacterial growth studies—are used to characterize mutants of MscL. Methods have been developed for either *in vivo* or *in vitro* investigation by patch clamp [18]. For *in vivo*, bacterial cells expressing MscL are enlarged to form giant spheroplasts, allowing for patch-clamp analysis. For *in vitro*, membrane proteins isolated from bacterial preparations are reconstituted into liposomes, which form unilamellar blisters under appropriate conditions that are also suitable for patch clamping. Patch clamping is very useful

because it allows for the direct measurement of the conductance of the channels, the observation of channel opening and closing events (and therefore, kinetic analysis), and determination of the tension applied to the membrane required for channel gating [7, 17, 19]. However, spheroplast and liposome preparations are technically challenging and time consuming, making this technique impractical as a high-throughput screen.

Bacterial growth studies take less time than patch-clamping techniques and are usually the best method available for characterizing mutants [9, 20, 21]. Gain-of-function (GOF) MscL mutants either gate at lower tensions than wild type or have increased spontaneous openings, and therefore are more leaky. Since leaky channels release important intracellular materials, cells expressing GOF mutants do not grow as well as those expressing wild-type MscL in normal culture conditions. Loss-of-function (LOF) MscL mutants require more tension to open them. Hence they do not provide as adequate a defense against downshock as does wild type, and LOF mutant bacteria are more likely to be killed when subjected to downshock.

Bacterial growth analysis is easier than patch clamping for screening but is still quite labor intensive and time consuming. In addition, bacterial growth assays are only suitable for MscL mutants produced *in vivo*. However, MscL has been synthesized chemically via solid-phase synthesis and native chemical ligation [22]. A high-throughput, cell-free assay would be superior to current techniques because it would allow for more rapid screening of mutants as well as characterization of mutants synthesized *in vitro*. One possibility for such an assay is a fluorescence-based technique to detect channel activity in synthetic vesicles.

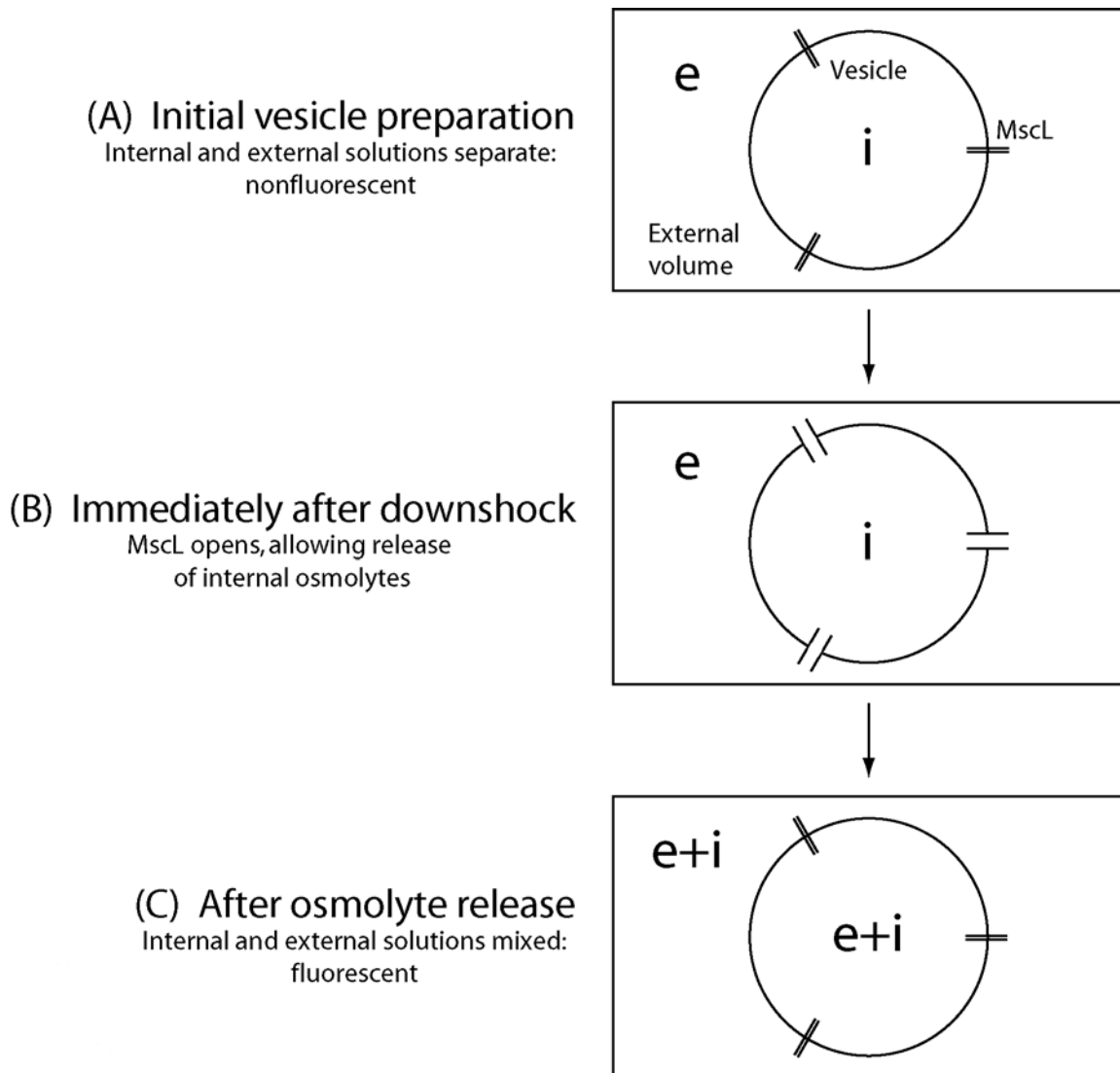


Fig. 3.3. Schematic of the proposed assay. The internal and external solutions, which are individually nonfluorescent but fluorescent when mixed, are *i* and *e*, respectively. The solutions are separate in the initial vesicle preparation (*A*), but MscL gating during downshock (*B*) opens pores in the membrane that allow the internal osmolytes to mix with the external solution (*C*).

The general scheme of the proposed fluorescence assay is outlined in fig. 3.3. The first step is the generation of a vesicle suspension that contains different solutions inside and outside the vesicles. Such a suspension can be easily prepared by forming vesicles in one solution and using gel filtration to exchange the external solution. We choose two solutions that are individually nonfluorescent but fluorescent in combination.

While the vesicles remain intact, the solutions are separate, and therefore the system is nonfluorescent. However, downshock of the vesicles results in the leakage of the interior solution (due to MscL activity or lysis) into the exterior solution, causing a sudden increase in fluorescence. Although the assay cannot directly distinguish between MscL activity and membrane rupture, MscL activity is detectable from differences in the fluorescence responses of vesicle preparations with and without the protein.

Theoretical Descriptions of Downshocked Vesicles

Laplace's Law provides the relationship between the osmotic pressure difference Δp and tension t in the vesicle membrane:

$$t = \frac{1}{2}\Delta p r \quad (3.1)$$

where r is the vesicle radius [23]. The definition of Δp is

$$\Delta p = RT\Delta c = RTD \quad (3.2)$$

where R is the ideal gas constant, T the absolute temperature, and Δc the concentration difference between the solutions inside and outside the vesicle. This equation also defines the downshock D as the concentration difference Δc . From Eq. (3.1) and Eq. (3.2), it is clear that for vesicles of a given radius, the tension is directly proportional to the downshock D .

The guiding principle of this assay is that the bilayer of a vesicle has a threshold tension, t_{thresh} , the maximum tension that it can withstand, dependent on its composition [23]. Eqs. (3.1) and (3.2) allow for the determination of the threshold downshock, D_{thresh} , corresponding to this tension. When downshocks less than D_{thresh} are applied, the vesicle remains intact. However, for greater downshocks, pores form in the vesicle, and it

releases some of its osmolytes. The release continues until the difference between the concentrations of the internal and external solutions is reduced to D_{thresh} , the largest downshock that allows the vesicle to survive intact. Fluorescence can be used to determine the fraction of the osmolytes released by the vesicles as a function of the applied downshock. This relationship allows for the determination of D_{thresh} for a preparation of vesicles.

The simplest model for this system (fig. 3.4A) consists of a uniform, spherical vesicle population with a total internal volume V_i and osmolyte concentration of $c_{i,init}$. If

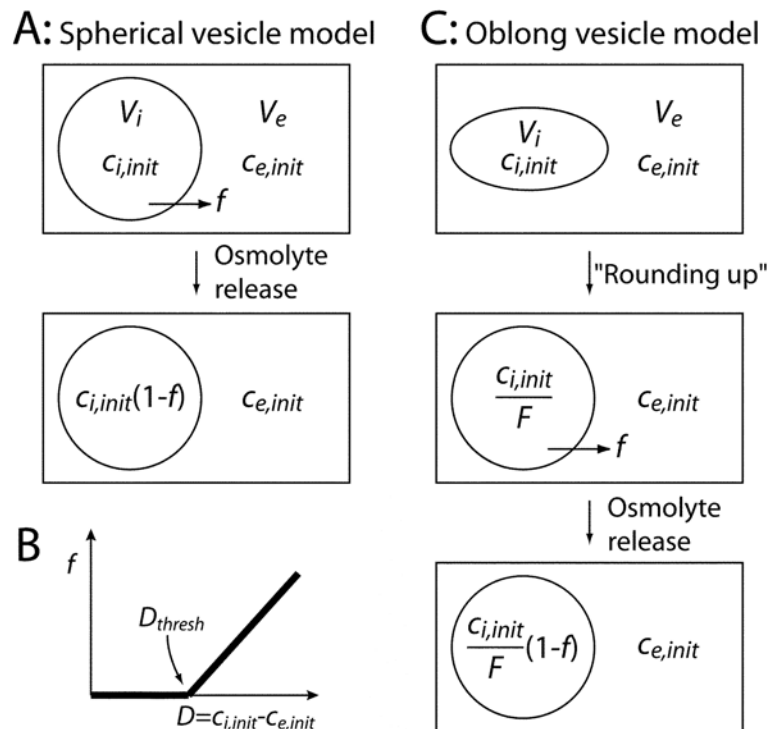


Fig. 3.4. Schematic of the models for vesicles experiencing downshock.

A, The spherical vesicle model. In an applied downshock, osmolyte release from the vesicle (circle) into the external volume changes the internal, and to a much lesser extent, the external concentrations. B, The expected function when the fraction of osmolytes released (f) is plotted against the applied downshock (D). The x -intercept of the sloped line is the threshold downshock D_{thresh} in the spherical vesicle model. C, The oblong vesicle model. The first response of an oblong vesicle (ellipse) experiencing downshock is to “round up” into a sphere. Only after this initial step are the osmolytes released as in A. The variables are explained in the text.

the number of vesicles is relatively small, V_i is much smaller than the external volume, V_e . Downshock occurs when the external osmolyte concentration is reduced to a value $c_{e,init}$ that is lower than $c_{i,init}$. The value of the applied downshock D is the initial difference between internal and external concentrations:

$$D = c_{i,init} - c_{e,init}. \quad (3.3)$$

If $D < D_{thresh}$, by definition, then no osmolytes are released, because the bilayer is strong enough to withstand the downshock. However, if $D > D_{thresh}$, then osmolytes are released. Let f be the fraction of the total intravesicular osmolyte concentration that is released from the vesicles upon downshock. The intravesicular concentration is reduced because of the outward flow of osmolytes, but the external concentration is negligibly affected because the external volume is so large compared to the internal volume.

Therefore, the final internal and external concentrations are

$$c_{i,final} = c_{i,init}(1 - f) \quad (3.4a)$$

$$c_{e,final} = c_{e,init} \quad (3.4b)$$

and the final concentration difference must be equivalent to D_{thresh} .

$$D_{thresh} = c_{i,final} - c_{e,final} \quad (3.5)$$

Combining Eqs. (3.4a), (3.4b), and (3.5) and rearranging gives

$$D_{thresh} = c_{i,init}(1 - f) - c_{e,init} \quad (3.6)$$

$$D_{thresh} = (c_{i,init} - c_{e,init}) - fc_{i,init}. \quad (3.7)$$

Combining Eqs. (3.3) and (3.7) gives

$$D_{thresh} = D - fc_{i,init}. \quad (3.8)$$

Rearranging Eq. (3.8) gives

$$f(D) = \frac{1}{c_{i,init}} D - \frac{D_{thresh}}{c_{i,init}} = mD + b \quad (3.9)$$

$$c_{i,init} = m^{-1} \quad (3.10a)$$

$$D_{thresh} = -\frac{b}{m}. \quad (3.10b)$$

The value of f must be 0 for all $D < D_{thresh}$. However, Eq. (3.9) indicates that for $D > D_{thresh}$, plotting f as a function of D should give a linear plot (fig. 3.4B). The slope m should be the reciprocal of the initial internal osmolyte concentration [Eq. (3.10a)]. D_{thresh} , which is the x -intercept of the line (fig. 3.4B), can be determined from the slope and y -intercept [Eq. (3.10b)].

A more complicated model (fig. 3.4C) also must be addressed. Vesicles prepared under some conditions are oblong, not spherical [24, 25]. In these cases, the first response of vesicles undergoing downshock is to “round up” into spheres, increasing their internal volume, and thus reducing their internal osmolyte concentration with no increase in membrane tension. The effective downshock is the difference between the *new* internal concentration and the external concentration. Let F be the factor by which the volume increases by “rounding up” (requiring $F > 1$). If the effective downshock after “rounding up” is large enough, the osmolytes are released, as in the first model. The definition of applied downshock [Eq. (3.3)] and the relationship between $c_{e,init}$ and $c_{e,final}$ [Eq. (3.4b)] are the same as in the spherical model. However, because of the change in intravesicular concentration, Eq. (3.4a) does not apply. Instead,

$$c_{i,final} = \left(\frac{c_{i,init}}{F} \right) (1 - f). \quad (3.11)$$

Now, combining Eqs. (3.4b), (3.5), and (3.11) gives

$$D_{thresh} = \left(\frac{c_{i,init}}{F} \right) (1 - f) - c_{e,init}. \quad (3.12)$$

Combining Eqs. (3.3) and (3.12) and rearranging yields

$$f(D) = \frac{F}{c_{i,init}} D + \left(1 - F - \frac{FD_{thresh}}{c_{i,init}} \right) = mD + b \quad (3.13)$$

which is again a linear function of D that allows for the determination of F and D_{thresh} .

$$F = mc_{i,init} \quad (3.14a)$$

$$D_{thresh} = \frac{1 - b}{m} - c_{i,init} \quad (3.14b)$$

In contrast to the spherical vesicle model, the oblong vesicle model requires $c_{i,init}$ in the calculation of both F and D_{thresh} , as seen in Eqs. (3.14a) and (3.14b).

The threshold downshock D_{thresh} corresponds to the downshock at which pores form in the vesicle bilayer. For vesicles composed of lipid only (–MscL vesicles), this is the downshock at which membrane rupture occurs. However, for vesicles that contain MscL (+MscL vesicles), the threshold downshock may be quite different. In these vesicles, MscL responds to the increasing tension by gating, thus opening pores at a downshock distinct from that of membrane rupture. To develop the assay for MscL gating, we must find conditions that provide distinct values for D_{thresh} for vesicles with and without MscL.

There are a number of discrete steps in the process of developing this assay. First, the best method for generating a uniform vesicle population must be determined. Second, it must be demonstrated that MscL can be incorporated into the vesicle population. Third, the fluorophore system must be optimized. Last, the vesicle composition (type of lipid and amount of protein) must be optimized. Table 3.1 shows

Table 3.1. Acronyms, names, and chemical groups of lipids.

Acronym	Full name	Headgroup ^a	Chain 1	Chain 2
chol	Cholesterol	N/A	N/A	
DLinPC	1,2-dilinolenoyl- <i>sn</i> -glycero-3-phosphocholine	PC	18:3 ^b	
DLPC	1,2-dilauroyl- <i>sn</i> -glycero-3-phosphocholine	PC	12:0	
DOPC	1,2-dioleoyl- <i>sn</i> -glycero-3-phosphocholine	PC	18:1	
DPPC	1,2-dipalmitoyl- <i>sn</i> -glycero-3-phosphocholine	PC	16:0	
POPC	1-palmitoyl-2-oleoyl- <i>sn</i> -glycero-3-phosphocholine	PC	16:0	18:1
POPE	1-palmitoyl-2-oleoyl- <i>sn</i> -glycero-3-phosphoethanolamine	PE	16:0	18:1
POPS	1-palmitoyl-2-oleoyl- <i>sn</i> -glycero-3-(phospho-L-serine)	PS	16:0	18:1

^a The headgroups include phosphatidylcholine (PC), phosphatidylethanolamine (PE), and phosphatidylserine (PS). ^b The notation m:n describing acyl chains indicates the length of the carbon chain (m) and the number of unsaturated bonds (n). Diacyl lipids have the same chain at both positions.

the types of lipids that will be considered and their acronyms, which will be used in the text.

RESULTS AND DISCUSSION

Vesicle Preparation

Both models discussed above have the important assumption that the bilayer tension in all the vesicles undergoing downshock is nearly the same and that the tension is directly proportional to the applied downshock. However, Laplace's Law [Eq. (3.1)] indicates that the proportionality only holds if all the vesicles have the same radius. Larger vesicles experience a larger tension than smaller vesicles at the same downshock, presenting a significant complication to the models. Therefore, the success of the assay depends heavily on the ability to produce a vesicle population of uniform size. Furthermore, the vesicles must be unilamellar, because the presence of MscL on the interior bilayers of multilamellar vesicles may not be detectable and the behavior of multilamellar vesicles is not well understood.

There are three commonly used methods for producing small, unilamellar vesicles: sonication, dialysis, and extrusion [26]. Sonication, which uses high frequency sound waves to break up large vesicles, produces vesicles that are so small (~30 nm in diameter) that they are osmotically insensitive. Their lack of tension changes under osmotic stress makes them unsuitable for a MscL gating assay. Vesicle preparation by dialysis involves dissolution of lipids in an aqueous detergent solution and dialyzing away the detergent [27]. Only the lipid remains, forming a vesicle suspension, but the resulting size distribution is broad. Because of the drawbacks of sonication and dialysis, the superior choice is extrusion, the passage of a lipid suspension through a filter, squeezing large vesicles into smaller ones. Extrusion can generate vesicles with sizes larger than those produced by sonication (hundreds of nm in diameter) and more narrow in size distribution than dialysis [28].

Previous work has shown extrusion filters with smaller pore sizes generate a higher fraction of unilamellar vesicles and a narrower size distribution. Vesicles extruded through a filter with 100 nm pores were shown to be almost exclusively unilamellar, whereas pore sizes of 200 and 400 nm produced populations that had increasing numbers of multilamellar vesicles [29–31]. Furthermore, 100 nm pores produced a size distribution much narrower than that of 200 nm pores, and the size distributions from 400 and 600 nm pores were multimodal, with vesicle sizes spread over a wide range [29].

Therefore, the characteristics of a vesicle population extruded through 100 nm pores, which were the smallest commercially available, appeared best suited for the assay. To confirm the previously reported size and lamellarity results, DOPC vesicles

were prepared by extrusion through 100, 600, and 1000 nm pores and analyzed by several techniques.

Dynamic light scattering (DLS), which is commonly used to determine size distributions for small particles [25, 29, 32, 33], was attempted on the vesicle preparations. However, the results were unreliable. The distributions varied widely for different vesicle samples prepared with filters of the same pore size and even for identical samples diluted to different degrees.

Because of this inconsistency, electron microscopy (EM) was used instead of DLS [24]. Vesicles prepared by extrusion were imaged by EM (fig. 3.5A–C) and their size distributions were determined (fig. 3.5D–E). Surprisingly, the 100, 600, and 1000 nm filters all yielded distributions centered at a diameter of approximately 100 nm. However, the most important difference was found not in the major peak but in the number of large vesicles. No vesicle observed in the 100 nm preparation was larger than 460 nm, while the other preparations had many vesicles larger than this, including some as large as almost 1000 nm. In addition, the large vesicles in the 600 and 1000 nm preparations tended to be multilamellar, while practically none of the vesicles in the 100 nm preparation were multilamellar, as is evident in the images. EM of other 100 nm samples prepared for different purposes (immunogold-labeled and freeze-fractured, discussed below) also showed size distributions similar to that for 100 nm in this experiment, indicating the consistency of the vesicle populations prepared by extrusion.

Therefore, it was determined that extrusion through 100 nm pores does provide a reasonably uniform population of unilamellar vesicles, making this the best of all available techniques for vesicle preparation for the desired assay.

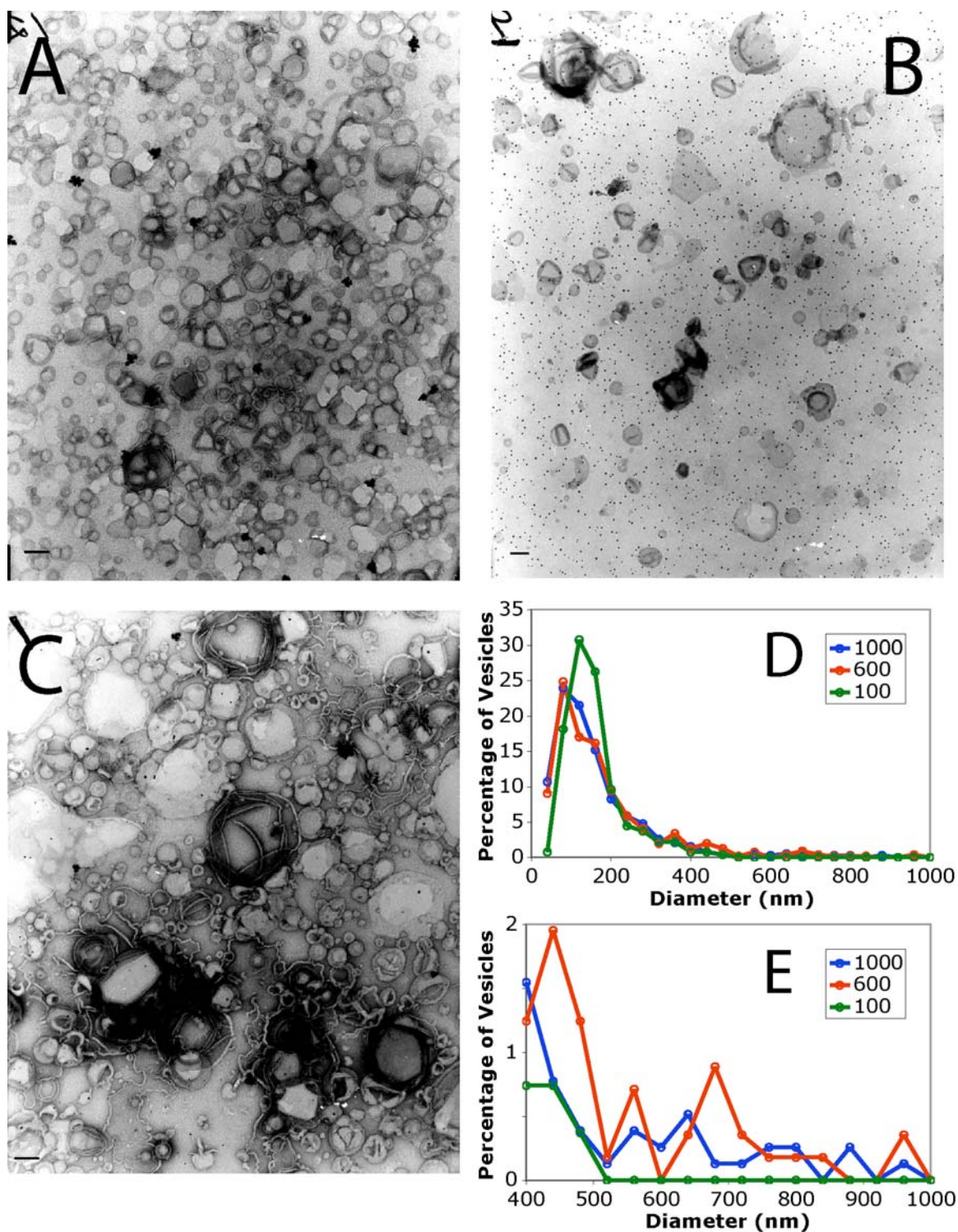


Fig. 3.5. Electron micrographs (A–C) and size distributions (D–E) of extruded vesicles. Representative micrographs showing vesicles extruded from filters with pores of 100 (A), 600 (B), and 1000 nm (C). Scale bars are 200 nm. D, The size distribution for each preparation determined from these and other images. E, An enlargement of the region with diameters greater than 400 nm. Data are the same as in D.

Verifying the Presence of MscL in Extruded Vesicles

It is extremely important to verify that MscL can be incorporated into vesicles prepared by extrusion. Therefore, MscL incorporation was verified by several different methods: Western blot, immunogold labeling, and freeze-fracture electron microscopy.

Western Blot

Because Western blotting is a standard technique for detecting small amounts of a protein with high specificity, it was the first method used to detect MscL in vesicles. In Western blotting, samples are separated during polyacrylamide gel electrophoresis (PAGE) and transferred to nitrocellulose paper, which is successively incubated with a primary antibody specific to the protein of interest and a secondary antibody specific for the primary antibody. The secondary antibody is conjugated to an easily detectable enzyme. Assaying the paper for the enzyme identifies the location of the protein of interest.

Extruded vesicles of DOPC (10 mg/mL) were prepared with and without MscL (100/1 lipid/protein) and purified by gel filtration to remove solubilized MscL from the external solution. PAGE was used to separate the components of each sample. Three lanes of each sample were run on the gel. Also, purified MscL solution was also run on the gel as a positive control; the total protein in the positive control lane was 1.5 μ g.

The protein in the gel was imaged by Western blot (fig. 3.6). The positive control showed a strong band of MscL monomer and a considerably weaker band of higher molecular weight, possibly MscL dimer (lane 1). The -MscL vesicle preparation contained no bands in any of the three lanes, as expected (lanes 5-7). The +MscL vesicle

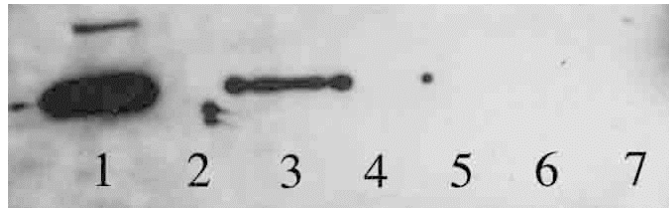


Fig. 3.6. Western blot of vesicles prepared with and without MscL. Lane 1: 1.5 μ g solubilized MscL. The MscL monomer is the large band, but a band of higher molecular weight is also present. Lanes 2–4: Vesicles prepared with MscL. Lanes 5–7: Vesicles prepared without MscL.

preparation did show a MscL band in lane 3, although it was significantly weaker than the positive control. In the other +MscL lanes (2 and 4), there were no MscL bands, but there were significant traces of MscL in both lanes as spots at the lane edge nearest to lane 3. The arrangement of the band and spots suggests that the MscL in lanes 2 and 4 is spillover from lane 3 during gel loading. Why the lanes did not all contain the same amount of protein is not clear. The fact that lane 3, not lane 2, contains the major band rules out the possibility that this band is due to spillover from misloading the positive control. Spillover would have resulted in more protein in lane 2 than lane 3. Therefore, the results suggested that at least some MscL was incorporated into the vesicles, but since there was some ambiguity, a second method for detecting incorporated MscL was used.

Immunogold Labeling

A different method to visualize MscL in vesicles is immunogold labeling. In this technique, the vesicle preparations are successively incubated with primary antibodies specific for the protein of interest and secondary antibodies specific for the primary antibody, which are covalently linked to a gold nanoparticle. Thus, the protein is labeled with a gold particle, observable by EM of the intact vesicles.

100 nm vesicles of DOPC with and without MscL were prepared by extrusion, incubated with different amounts of anti-6His mouse antibody, and then incubated with different amounts of Protein-G gold conjugate, which binds the mouse antibody. Our protein was expressed with a 6His tag at its N-terminus to simplify purification and labeling. –MscL vesicles as well as a +MscL preparation incubated without primary antibody but with Protein G represented negative controls for this experiment, because none of these vesicles was expected to bind gold particles. The final solutions were imaged by EM.

This procedure was performed several times, with different results. In some experiments, there was a clear gold labeling of the +MscL vesicles (fig. 3.7A–C). Almost all vesicles were labeled with one or more gold particles, and there were relatively few free gold particles. However, in other instances the labeling of the +MscL vesicles (fig. 3.7D) was no greater than that of the negative controls (fig. 3.7E–F). In these cases the gold particles appeared to be randomly distributed. The former results suggested the presence of MscL, but the latter suggested its absence.

Therefore, as seen in the Western blot, there is some evidence of MscL incorporation in the vesicles, but the ambiguity in the results necessitates a more definitive study.

Freeze-Fracture Electron Microscopy

Freeze-fracture EM is a definitive method for visualizing proteins embedded in membranes. Bilayers that have been flash-frozen are split relatively easily into their separate leaflets. Transmembrane proteins remain intact in one of the leaflets, resulting

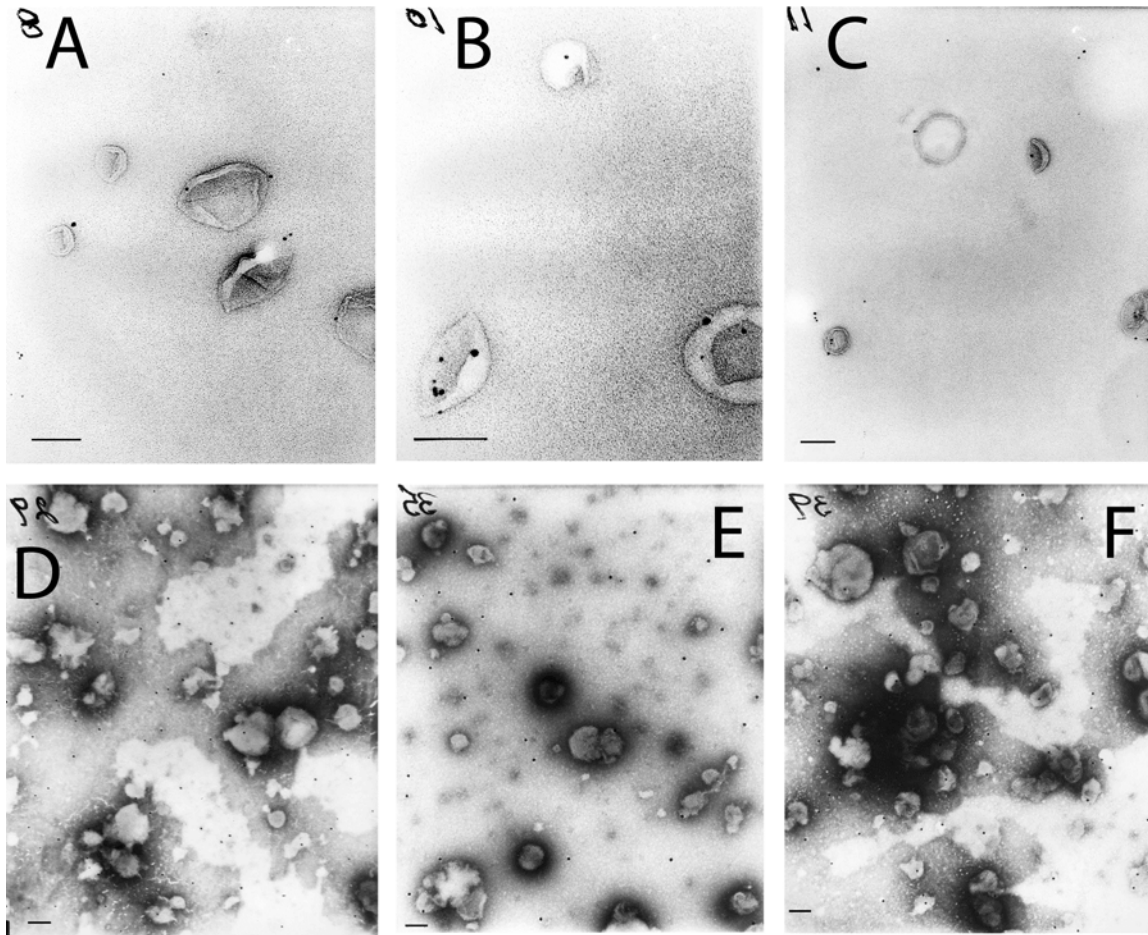


Fig. 3.7. Micrographs of immunogold-labeled vesicles. *A–C*, Representative micrographs from one experiment. All images contain +MscL vesicles labeled with 1° antibody and 2° antibody-gold particle conjugate. The small black dots are gold particles. *D–F*, Representative images from the same experiment performed later. *D*, +MscL vesicles labeled with 1° antibody and a 2° antibody-gold particle conjugate. *E*, –MscL vesicles with the same labeling. *F*, +MscL vesicles labeled with only 2° antibody-gold particle conjugate. The gold particles are associated with the vesicles in *A–C*, but in *D*, the distribution of the gold particles is no different from the negative controls *E–F*. All scale bars are 100 nm.

in a protrusion in one leaflet and a hole in the other. Visualization by EM reveals these defects.

100 nm DOPC vesicles with MscL were prepared by extrusion and analyzed by freeze-fracture EM. The images showed a large number of membrane defects likely due to protein particles in the vesicles (fig. 3.8). While a few vesicles did not contain any

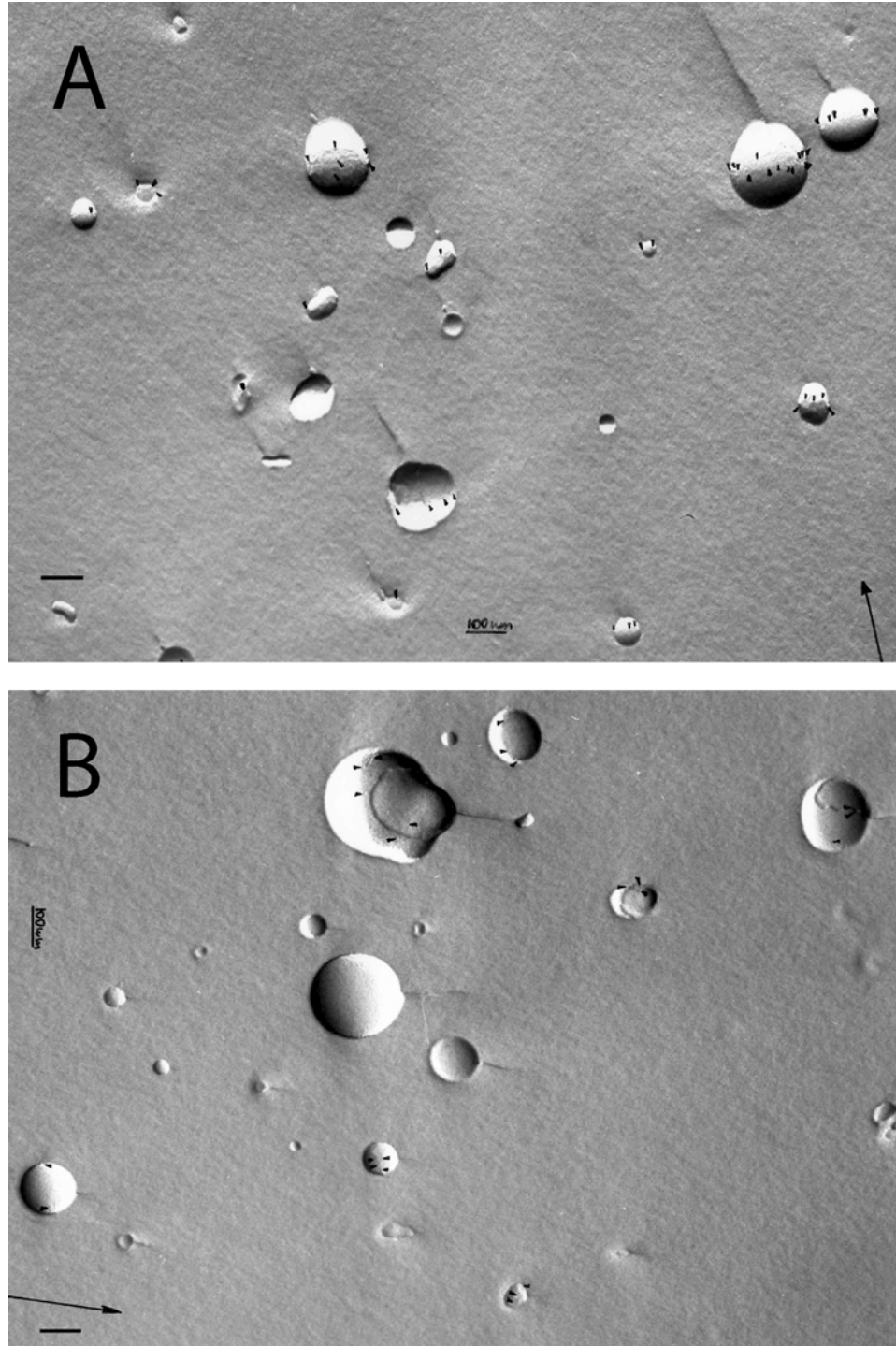


Fig. 3.8. Freeze-fracture electron micrographs of +MscL vesicles. Both images are from the same preparation. The small black arrowheads show probable protein locations. The arrows in the corners indicate the shadow direction. Scale bars are 100 nm.

visible defects, most vesicles contained more than one, with some containing more than ten.

The results here unambiguously indicated that MscL is incorporated in vesicles prepared by extrusion, laying the groundwork for further progress on the assay for MscL activity.

Evaluation of Fluorescence Systems

The assay requires solutions that are independently nonfluorescent but fluorescent when mixed (fig. 3.3). There are many solutions that satisfy this requirement, so we tried several to determine the optimal fluorescence system.

Certain fluorophores or ligands display large fluorescence increases upon binding metal ions, including fluo-3 with Tb^{3+} , calcium green 1 with Tb^{3+} or Cd^{2+} [34], and dipicolinic acid (DPA) with Tb^{3+} [35]. In principle, encapsulation of these fluorophores in vesicles and their subsequent release into an external solution of the metal ions results in a large fluorescence increase. DOPC vesicles with each of these fluorophores were prepared and tested for their usefulness in the assay. The Tb^{3+} /DPA system, which has been used in several biological applications such as endospore detection [36], vesicle fusion [37, 38], and vesicle leakage [38, 39], proved to be superior to the fluo-3 and calcium green 1 systems. The latter fluorophores are sensitive to calcium ions, and there were noticeable background signals due to calcium impurities in the intravesicular solution. The Tb^{3+} /DPA system is insensitive to other common ions, and therefore does not suffer from this complication. Vesicles encapsulating Tb^{3+} that were purified by gel

filtration to replace the external solution with one containing DPA were always free of background fluorescence.

Another system that was also considered involved carboxyfluorescein (CF), a self-quenching fluorophore, which has been used previously in several vesicle leakage assays [24, 40–42]. This molecule is highly fluorescent in dilute concentrations but self-quenching at very high concentrations [34]. Vesicles loaded with high concentrations of CF (100 mM) have no detectable fluorescence, but release from the vesicles results in a dilute, fluorescent external CF solution.

Because both the Tb^{3+} /DPA and CF systems met the requirements for this assay—two nonfluorescent solutions that increased in fluorescence on mixing—both of them were used. Early experiments utilized Tb^{3+} /DPA before CF was explored as an alternative. But later experiments used CF because it possessed two advantages over Tb^{3+} /DPA. First, gel filtration of the vesicles, an essential step that exchanges the extravascular solution, was easier for CF than for Tb^{3+} /DPA. Tb^{3+} and DPA are both colorless, but CF appears brown at high concentrations and green at low concentrations. Therefore, the progress of the vesicles and the free CF in the column could be followed much more easily. Second, in the absence of a chelator, Tb^{3+} has been shown to change the fluidity characteristics of phosphatidylserine (PS) when encapsulated in PS vesicles [37]. Citrate was used as a chelator in the experiments in order to minimize the association of Tb^{3+} with the lipids, but the use of CF avoided this complication entirely.

Optimization of Vesicle Composition—Lipid Composition

Using the optimized vesicle preparation technique and fluorescence systems, vesicles of various types of lipids were investigated in the downshock assay to optimize the lipid system. Ideally, the conditions should result in a large difference in the D_{thresh} values for +MscL and –MscL vesicles, requiring a lipid system with a large difference between the tensions for MscL gating and membrane rupture.

In general, much more is known about membrane rupture than MscL gating in different lipid types. The stability of pure bilayers strongly depends on the melting temperature (T_m) of the lipids [43]. The melting temperature, in turn, depends on the degree of unsaturation in the lipid tails [44, 45]. Lipids with unsaturated tails tend to have lower melting temperatures and are more easily ruptured, while saturated lipids can generally withstand higher membrane tensions.

In contrast, there is very little experimental data on the gating behavior of MscL in different lipid environments. Patch-clamping experiments on MscL have been performed in only two lipid environments, the natural bacterial membrane and the lipid mixture soybean azolectin [18]. Also, while there is a working model for the MscL gating mechanism and the protein/lipid interactions involved [3, 46], it is still relatively unsophisticated. It does not detail any specific roles for the headgroups or unsaturation in the lipid tails.

To complicate matters further, tensions in membranes are not straightforward to determine experimentally, as they depend on both the pressure and the radius of curvature [Laplace's Law, Eq. (3.1)]. In short, it was impossible to predict *a priori* the lipid system

Lipid	T_m (°C)	Ref.
DLinPC	-60	44
DOPC	-20	44
POPC	-2	44
80/20 DOPC/DPPC	12	45
40/60 DOPC/DPPC	30	45

Table 3.2. Melting temperatures (T_m) of lipids and lipid mixtures.

that provides the best conditions for this assay. Therefore, many lipids were tested to determine the optimal lipid or mixture by trial and error.

Membrane Fluidity

First, vesicles were prepared of lipids and lipid mixtures across a broad range of melting temperatures, which are summarized in table 3.2. 100 nm vesicles with and without MscL (1000/1 lipid/protein) were prepared in CF rehydration buffer, and the external solution was replaced with exchange buffer by gel filtration. The vesicle preparations were subjected to a serial downshock protocol.

The data are summarized in fig. 3.9. Each plot of the fraction of osmolytes released versus the downshock had the shape predicted by the theoretical models: very little release of osmolytes for all downshocks less than some threshold, and a linear release for greater downshocks (fig. 3.9A–E). The lines of best fit were determined for the linear release for each vesicle sample, which allowed for the determination of D_{thresh} and other parameters, according to the above equations describing the two models. The data are summarized in table 3.3.

The results indicated that the oblong vesicle model was not an accurate description of the system. The results contradict the model's assumption that the vesicles increase their net volume by "rounding up" in response to osmotic downshock. If

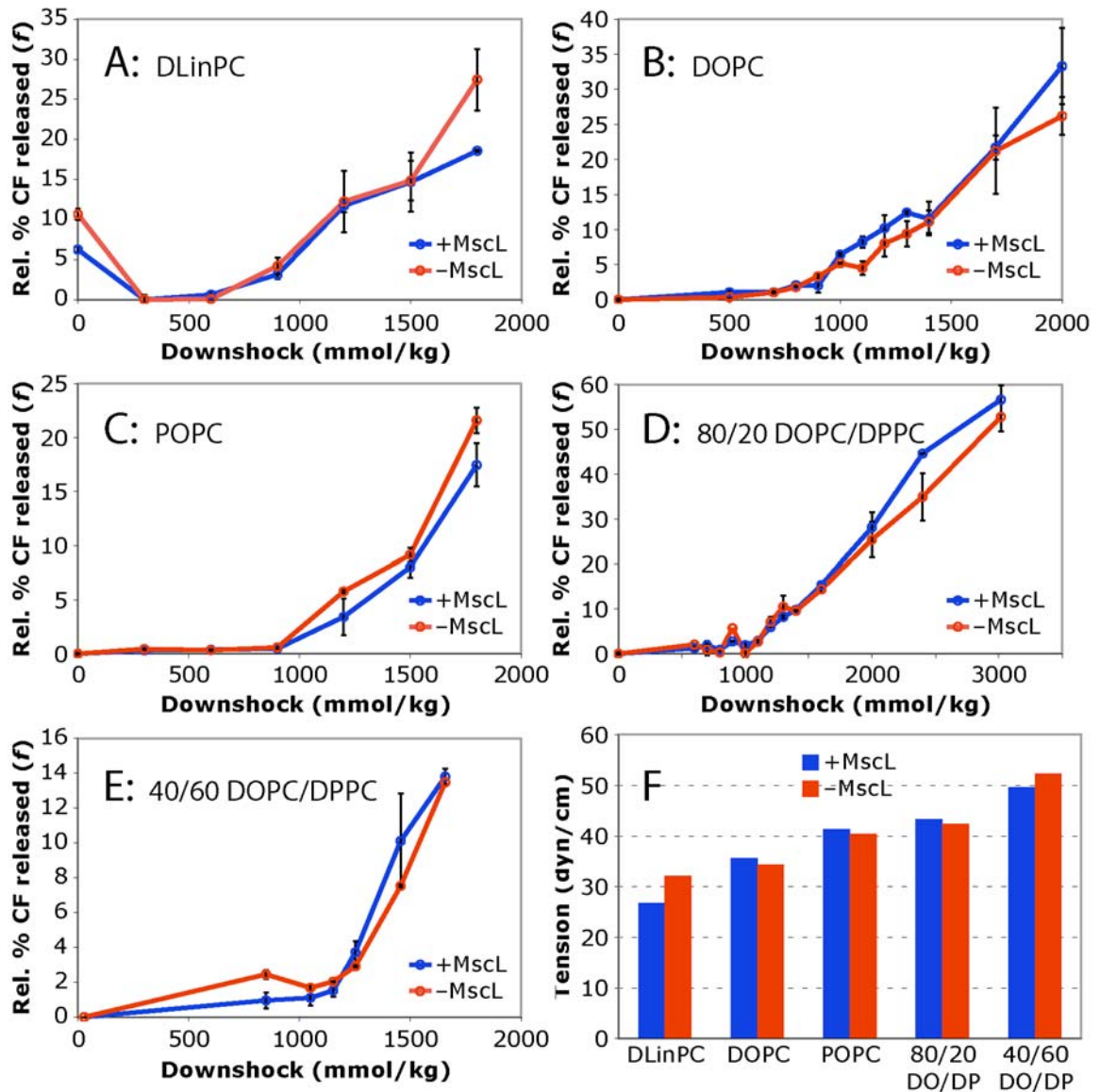


Fig. 3.9. Fraction of released osmolytes versus applied downshock for lipid mixtures with different melting temperatures. *A*, DLinPC. *B*, DOPC. *C*, POPC. *D*, 80/20 (m/m) DOPC/DPPC. *E*, 40/60 (m/m) DOPC/DPPC. *F*, The calculated threshold tensions for osmolyte release for each vesicle preparation. As expected, the tensions increase monotonically with the lipid T_m , but there are no appreciable differences between the tensions for the vesicles with and without MscL for each lipid. Error bars in *A–E* are the standard errors of the mean.

“rounding up” occurred, then the parameter F , which is the factor by which the volume increases, must be greater than 1. However, the analysis of all vesicles samples gave a value of F of less than 1, by a significant amount in most cases, implying a decrease in

Table 3.3. Analysis of serial downshock experiments, varying the lipid.

Vesicle Composition		m	b	Oblong Vesicle Model		Spherical Vesicle Model			
				F	D_{thresh} mmol/kg	Calc. $c_{i,init}$ mmol/kg	D_{thresh} mmol/kg	% Diff $c_{i,init}$	t_{thresh} dyn/cm
DLinPC	+	0.0164	-10.129	0.525	3520	6100	618	90.5	26.8
	-	0.0241	-17.868	0.771	1690	4150	741	29.7	32.1
DOPC	+	0.0262	-21.554	0.838	1440	3820	823	19.3	35.7
	-	0.0212	-16.807	0.678	2310	4720	793	47.4	34.4
POPC	+	0.0185	-17.634	0.592	3160	5410	953	68.9	41.3
	-	0.0221	-20.619	0.707	2260	4530	933	41.4	40.4
80/20 DOPC/DPPC	+	0.0289	-28.883	0.925	1260	3460	999	8.13	43.3
	-	0.0253	-24.747	0.810	1730	3950	978	23.5	42.4
40/60 DOPC/DPPC	+	0.0251	-27.347	0.803	1870	3980	1090	24.5	49.6
	-	0.0261	-29.986	0.835	1780	3830	1150	19.7	52.3
55/45 POPC/chol	+	0.0164	-12.406	0.525	3650	6100	756	90.5	32.8
	-	0.0181	-12.029	0.579	2990	5520	665	72.7	28.8
37/33/30 DOPC/ DPPC/chol	+	0.0262	-20.970	0.838	1420	3820	800	19.3	34.7
	-	0.0237	-19.275	0.758	1830	4220	813	31.9	35.3

The + and – signs indicate the presence or absence of MscL. m , b , F , D_{thresh} , $c_{i,init}$, and t_{thresh} are defined in the text in the theoretical description of the vesicle models; calc. $c_{i,init}$ is the value of $c_{i,init}$ calculated from Eq. (3.10a); % diff. $c_{i,init}$ is the percent difference between this calculated value and the actual $c_{i,init}$; t_{thresh} is calculated from D_{thresh} and Eqs. (3.1) and (3.2), assuming a vesicle diameter of 100 nm.

the effective volume of the vesicles. It is counterintuitive that vesicles experiencing downshock would shrink, and it is incompatible with the model.

Analysis by the spherical vesicle model, on the other hand, gave more intuitive results. First, the model states that the reciprocal of the slope is the initial intravesicular osmolality. The errors in the predicted osmolality from the actual value (~3200 mmol/kg) are reasonably low (within 30%) in most cases, and there are legitimate reasons for the large errors. Specifically, the lines for the POPC vesicle samples were drawn from only three data points each, the fewest of any sample, so the error in the slopes may have been reduced with more data. Also, the line for the DLinPC +MscL sample was most likely skewed by the data point at 1800 mmol/kg, which does not fit very well with the rest of the DLinPC data. Second, the values for the threshold tension

as calculated by this model increase monotonically with the lipid T_m (fig. 3.9F), which agrees with the literature [44]. Furthermore, these tensions are not far from the 40 dyn/cm tension threshold determined previously for several lipid mixtures [24, 47], although other reports claim significantly lower tension thresholds [32, 43].

For these reasons, the values for D_{thresh} from analysis by the spherical vesicle model are the values reported for the vesicle samples. Unfortunately, none of the lipids display significant differences in D_{thresh} for +MscL and -MscL vesicles, which is not surprising given the way the plots for all lipids overlay each other.

Further experiments were performed using mixtures of lipids and cholesterol, which stiffens membranes and alters their fluidity properties. Experiments were performed exactly as above, except the lipid mixtures were 55/45 POPC/chol and 37/33/30 DOPC/DPPC/chol. The results (fig. 3.10 and table 3.3), as before, show no appreciable differences between +MscL and -MscL vesicles. Thus, using a series of lipids and lipid mixtures with different membrane fluidities failed to provide a lipid system that could differentiate the activity of MscL from membrane rupture.

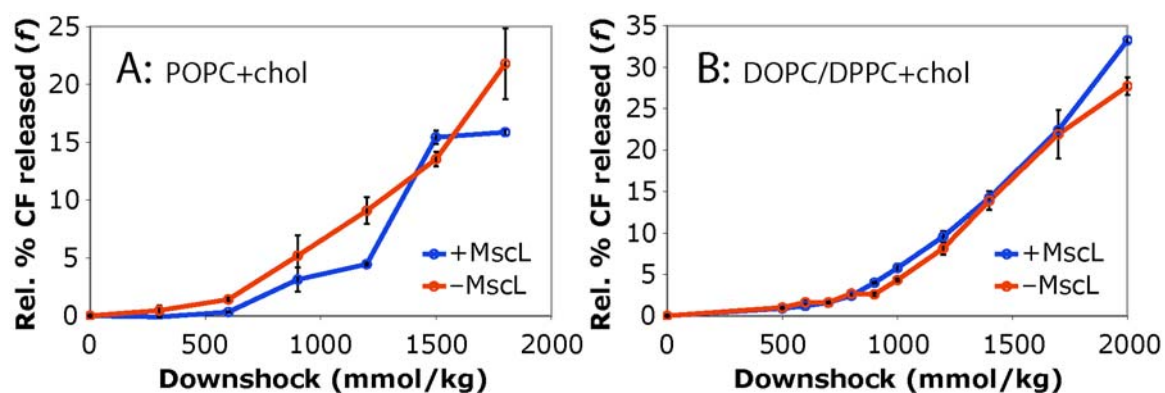


Fig. 3.10. Fraction of released osmolytes versus applied downshock for lipid mixtures containing cholesterol. *A*, 55/45 (m/m) POPC/chol. *B*, 37/33/30 (m/m) DOPC/DPPC/chol. There are no appreciable differences for vesicles with and without MscL. Error bars are standard errors of the mean.

Shorter Lipid Tails

Previous work has shown that MscL has a lower gating tension in lipids with shorter lipid tails [48, 49]. For this reason, +MscL and –MscL vesicles were prepared with DLPC as above. This lipid was found to be unsuitable for the assay because the intravesicular volume after extrusion was very low. It is not clear if this is because the vesicles are very small or few in number. In either case, because of the low signals that resulted from downshock, the data were too noisy to be rigorously analyzed.

Different Headgroups

Lipids with different headgroups—POPS and 50/50 POPE/POPS—were used in the preparation of vesicles with and without MscL, as above, except the fluorescence system chosen was Tb³⁺/DPA instead of CF. These lipids were found to be unsuitable, however, because the vesicles of these compositions were leaky. Even in the absence of any downshock whatsoever, a large amount of background fluorescence was observed. It is not clear why the contents leaked from the vesicles, but such leakage is incompatible with the assay.

Natural Lipid Mixtures

Two natural lipid mixtures, soybean azolectin and *E. coli* membrane extract, were also used. These mixtures were chosen because MscL reconstituted into azolectin has been used in all *in vitro* patch-clamp experiments [18], and the membrane extract from *E. coli* provides as close a match as possible to the native environment of MscL. Vesicles of

these lipid mixtures were prepared with and without MscL as above to determine their suitability for the assay.

The downshock results for +MscL and –MscL vesicles of azolectin, which consists of a mixture of various diacylphosphatidylcholines, were indistinguishable, as seen for all previous lipid systems, and therefore provided no advantage for the assay.

Vesicles prepared from *E. coli* extract, which consists of 57.5% phosphatidylethanolamine, 15.1% phosphatidylglycerol, 9.8% cardiolipin, and 17.6% other lipids, were unsuitable because of problems with their purification. When purified using gel filtration, they became stuck in the column, never eluting. This occurred using beads of two different materials, Sephadex (dextran) and Biogel (polyacrylamide). Purification of the vesicles was also attempted using dialysis, but this was prohibitively time consuming. Using small volume dialyzers to perform the dialysis, there was only partial buffer exchange even after 72 hours. Because the exchange of the external solutions is an absolute requirement for the assay, *E. coli* extract could not be used.

Optimization of Vesicle Composition—Protein Amount

It is possible, although unlikely, that the downshock assay could not detect MscL activity because a lipid/protein ratio of 1000/1 results in only a few channels in each vesicle. The freeze-fracture EM images indicated that many vesicles had only two or three channels (fig. 3.8). Therefore, the effects of using different amounts of protein were also explored.

DOPC vesicles were prepared with lipid/protein ratios of 2000/1, 1000/1, and 400/1, and with no protein, purified, and subjected to a serial downshock protocol.

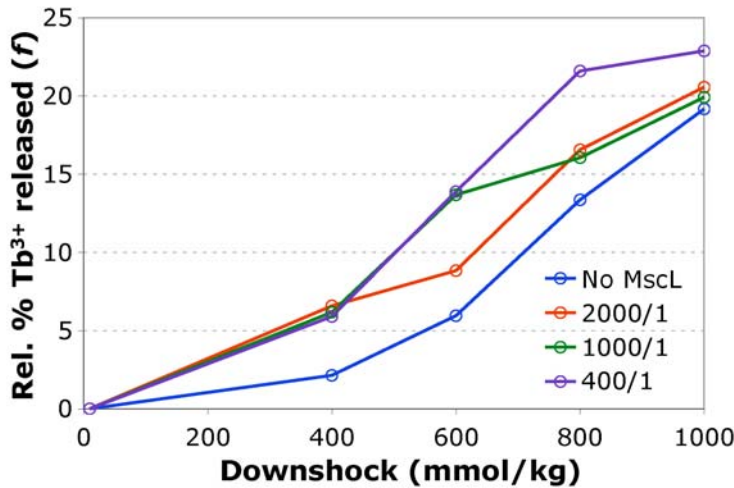


Fig. 3.11. Fraction of released osmolytes versus applied downshock for vesicles containing different amounts of protein. The lipid/protein ratio for each sample is given.

Tb³⁺/DPA instead of CF was used for this experiment. The results are shown in fig. 3.11 and table 3.4.

The data in this experiment appear to indicate that vesicles with any amount of MscL have lower D_{thresh} values than –MscL vesicles. However, the D_{thresh} values for the 1000/1 and –MscL samples differ significantly from those observed in previous experiments (table 3.3). Because the previous data fit with the expected relationship between threshold tensions and T_m , these results are probably not quantitatively accurate. However, the key finding is that having more or less MscL than in the previous experiments did not alter the D_{thresh} value substantially.

Table 3.4. Spherical vesicle model analysis of serial downshock experiments, varying the amount of protein

Lipid/Protein	m	b	Calc. $c_{i,init}$ mmol/kg	D_{thresh} mmol/kg
400/1	0.0293	–4.4603	3410	152
1000/1	0.0218	–1.3126	4590	60.2
2000/1	0.0248	–4.2538	4030	172
No MscL	0.0292	–10.315	3420	353

In summary, no vesicle composition tested produced vesicles that allowed for the detection of MscL activity. For some lipids, the vesicles could not even be produced and purified, as required for the assay. For others, the expected decrease in the downshock threshold values of vesicles with MscL compared to those without MscL was not observed. Also, changing the amount of MscL did not lead to this decrease, either.

CONCLUSION

The development of a high-throughput fluorescence-based assay for MscL activity involved several steps: determining the optimal method for vesicle formation, assuring the presence of MscL in vesicles prepared by this method, determining the optimal fluorescence system, and finding a vesicle composition that allows for MscL detection under downshock conditions. However, the final goal of detecting MscL activity was never met. There are two main possible reasons for the failure of this assay.

The simplest explanation is that MscL was never incorporated into the vesicles. If this were true, then the alleged +MscL vesicle samples were actually no different from the –MscL samples, and it is not surprising that the downshock results never reported any difference. However, this is improbable. While detection of MscL in the vesicles samples by Western blot and immunogold staining was somewhat ambiguous, the most rigorous detection technique—freeze-fracture EM—supported MscL incorporation. Furthermore, the method utilized here has been used previously to reconstitute MscL for patch clamp experiments on larger vesicles, which indisputably demonstrated MscL incorporation [50].

The more likely explanation for the failure of the assay is the inability to produce a sufficiently uniform vesicle sample. The uniformity demanded by an assay for MscL gating may be unattainable by current techniques for producing vesicles. Because the gating tension for MscL is relatively close to the membrane lysis tension, and tension depends directly on the vesicle radius, both phenomena may occur at the same downshock within a population of vesicles, even with a narrow size distribution. Even extrusion through 100 nm pores, the best technique for producing vesicles, resulted in a distribution with a full-width, half-maximum of about 100 nm, and almost 5% of the vesicles had diameters of more than 300 nm (fig. 3.5D–E).

The fact that extrusion may produce a vesicle population that varies not just in size, but in shape as well, is a further complication [24]. The failure of the oblong vesicle model presented earlier to adequately describe the experimental vesicle system does not imply that oblong vesicles do not exist. It is possible that the flaw in the model comes from the oversimplifying assumption that all oblong vesicles are produced with the same ratio of surface area to volume.

It was determined that this project was not worth continuing for two reasons. First, the development of a vesicle-based assay for MscL activity must wait for the development of better techniques for producing uniform vesicle populations. Given the current techniques, no further progress could be made. Second, a separate fluorescence-based bacterial growth assay for screening MscL mutants was developed that rendered the vesicle-based assay obsolete [51]. The only application requiring a vesicle-based assay was the screening of chemically synthesized MscL mutants, and although MscL has been chemically synthesized previously, it is not an area of current research.

MATERIALS AND METHODS

Materials

Most lipids (dissolved in chloroform at concentrations of 20–25 mg/mL), the Mini-Extruder, and the extruder heating block were purchased from Avanti Polar Lipids (Alabaster, AL). Soybean azolectin was purchased from Sigma as a lyophilized powder and was dissolved in chloroform to a concentration of 25 mg/mL before use. Sucrose, NaCl, KCl, and sodium citrate were purchased from Mallinckrodt (St. Louis, MO). MOPS, cholic acid, DPA, and Sephadex G-50 (fine grade) were purchased from Sigma. Carboxyfluorescein (CF) was purchased from Molecular Probes (Eugene, OR). TbCl_3 was purchased from Fluka. Mouse anti-6His antibody was purchased from Covance/BAbCo, and the Protein G-gold conjugate was purchased from BBIInternational (Cardiff, Wales). Purified *E. coli* MscL protein was a generous gift from the lab of Douglas Rees [15]. The protein, solubilized in 0.05% β -dodecylmaltoside (DDM), had a concentration of approximately 15 mg/mL. There was a 6His tag at its N-terminus so that it could be easily purified and labeled.

For the CF fluorescence system, high osmolality exchange buffer contained 1000 mM sucrose, 950 mM NaCl, and 10 mM MOPS, pH 7.8. High osmolality rehydration buffer contained 1000 mM sucrose, 750 mM NaCl, 100 mM CF, and 10 mM MOPS, pH 7.8. The osmolalities of the exchange and rehydration buffers were matched at ~3200 mmol/kg. Low osmolality downshock buffer contained only 10 mM MOPS, pH 7.8 (osmolality 30 mmol/kg). Detergent buffer consisted of 20 mM cholic acid in high osmolality exchange buffer. For the Tb^{3+} /DPA fluorescence system, high osmolality rehydration buffer contained 18 mM TbCl_3 , 180 mM sodium citrate, 600 mM

sucrose, and 10 mM MOPS, pH 7.2. High osmolality exchange buffer contained 3 mM DPA, 800 mM sucrose, 100 mM KCl, and 10 mM MOPS, pH 7.2. The osmolalities were matched at ~1200 mmol/kg. Low osmolality downshock buffer contained 3 mM DPA and 10 mM MOPS, pH 7.2 (osmolality 38 mmol/kg). Detergent buffer consisted of 20 mM cholic acid in high osmolality exchange buffer.

Vesicle Preparation

750 μ L of lipid solution (15 mg total lipid) was placed in a round-bottom flask. The chloroform was removed by rotary evaporation to yield a thin lipid film on the flask bottom. The film was dried further under high vacuum for 8–12 hours. For vesicle preparations with MscL, 1 μ L of MscL solution (~15 μ g, a 1000/1 lipid/protein ratio) was applied to the dried lipid and agitated to reconstitute the protein in the lipid molecules. Other ratios were sometimes used, as indicated in the text. For vesicle preparations without MscL, 1 μ L of 0.05% DDM solution was applied as a control for the DDM in the MscL solution. The lipid film (or lipid/protein mixture) was rehydrated in 5 mL rehydration buffer, giving a lipid concentration of 3 mg/mL in the final suspension. For vesicles that were produced for purposes other than downshock (e.g., electron microscopy), exchange buffer was used instead of rehydration buffer. The flask was agitated until all the lipid was removed from the side of the flask and rehydrated in the buffer, and the suspension was subjected to 3–5 freeze-thaw cycles at -80 °C. Extrusion was performed using the Avanti Mini-Extruder. 1 mL of the suspension was pulled into one of the pair of extruder syringes and passed back and forth 31 times through a polycarbonate filter with pore sizes of 100, 600, or 1000 nm. For lipids that have a T_m

higher than room temperature, the rehydration and extrusion were carried out in the extruder heating block at 50 °C to maintain fluidity.

Gel filtration was used to exchange the solution outside the vesicles. A gel filtration column of fine grade Sephadex G-50 was prepared in exchange buffer with a bed volume about ~10 mL. As the vesicle suspension passed through the column, the vesicles remained in the void volume and were eluted more quickly than the solutes that were free in solution. The vesicle suspension eluted from the column still had rehydration buffer inside, but now had exchange buffer outside. After the application of the vesicle suspension, at least five bed volumes of exchange buffer were flowed through the filtration column to eliminate all traces of the rehydration buffer.

Electron Microscopy

Vesicles were prepared in exchange buffer. A drop of vesicle suspension was placed in a charged gold grid and allowed to sit for 30 seconds. The solution was then dried from the grid by dabbing with the corner of a slice of filter paper. The dried grid was stained with uranyl acid or phosphotungstic acid solution, which was also allowed to sit for 30 seconds before the solution was dried by the same method. The grids were imaged with a scanning electron microscope.

Freeze-fracture EM was performed at Nano Analytical Laboratory (San Francisco, CA).

Immunogold Labeling

Vesicles with and without MscL were prepared in exchange buffer. 300 μL of +MscL vesicle suspension were incubated with 0, 0.3, or 0.6 μL primary antibody solution (0, 1/1000, or 1/500 dilutions). The 1/500 sample was prepared in duplicate. The incubation times were 45 minutes and 75 minutes for the 1/500 and 1/1000 samples, respectively. The primary antibody was a mouse IgG monoclonal antibody specific for the 6His tag, which the protein has at its N-terminus. After incubation, the vesicle samples were purified of unbound antibody by gel filtration. 300 μL of the three vesicle samples were incubated with 6 μL secondary antibody (1/50 dilution) for 45 minutes. In addition, the second 1/500 dilution sample was incubated with 3 μL secondary antibody (1/100 dilution) for 75 minutes. The secondary antibody was Protein-G conjugated to a 10 nm gold particle. As a negative control, -MscL vesicles were also incubated with a 1/500 dilution of primary antibody followed by 1/50 dilution of secondary antibody, as above.

Serial Downshock Protocol

High osmolality exchange buffer and low osmolality downshock buffer were mixed in various proportions to produce solutions of intermediate osmolalities. 5 μL of the purified vesicle preparations were subjected to downshock by dilution in 195 μL of these intermediate solutions in a 96-well plate. In addition, 5 μL of the purified vesicle preparations were also applied to 195 μL detergent buffer, which dissolved the lipids and freed the encapsulated osmolytes. A SpectraMax Gemini XS fluorescence plate reader (Molecular Devices, Sunnyvale, CA) using SOFTmax PRO 3.1.2 software was used to

measure the fluorescence of each sample for 60 minutes, allowing the fluorescence to stabilize. For the CF fluorescence system, the excitation wavelength was 492 nm, and emitted light was filtered at 515 nm and read at 520 nm with low PMT sensitivity. For the Tb³⁺/DPA fluorescence system, the excitation and emission wavelengths were 287 and 544 nm, respectively, and medium PMT sensitivity was used.

Data Analysis

Each raw fluorescence measurement was converted to a fluorophore concentration by comparison with standard curves. For each downshocked sample, the ratio of the fluorophore concentration to that of the corresponding detergent-treated sample was calculated to determine the fraction of the osmolytes released during downshock. The relative released fraction for each sample was determined by subtracting the minimum value for the downshock series. The relative released fraction was then plotted as a function of the applied downshock and analyzed according to the spherical and oblong vesicle models.

It should be noted that in experiments using the CF fluorescence system, after treatment with detergent, the CF concentrations ranged from 1 to 5 μM . This represents a 10^4 - to 10^5 -fold dilution of the initial intravesicular CF concentration of 100 mM. Therefore, the total volume of the solution is 10^4 - to 10^5 -fold greater than the intravesicular volume, which justifies the assumption of Eq. (3.4b) that the intravesicular volume is negligible compared to the external volume.

REFERENCES

1. Martinac, B. 2004. Mechanosensitive ion channels: Molecules of mechanotransduction. *J. Cell Sci.* 117:2449-2460.
2. Strop, P., R. Bass, and D. C. Rees. 2003. Prokaryotic mechanosensitive channels. *Adv. Protein Chem.* 63:177-209.
3. Hamill, O. P., and B. Martinac. 2001. Molecular basis of mechanotransduction in living cells. *Physiol. Rev.* 81:685-740.
4. Sukharev, S. I., P. Blount, B. Martinac, and C. Kung. 1997. Mechanosensitive channels of *Escherichia coli*: The MscL gene, protein, and activities. *Annu. Rev. Physiol.* 59:633-657.
5. Berrier, C., M. Besnard, B. Ajouz, A. Coulombe, and A. Ghazi. 1996. Multiple mechanosensitive ion channels from *Escherichia coli*, activated at different thresholds of applied pressure. *J. Membr. Biol.* 151:175-187.
6. Levina, N., S. Totemeyer, N. R. Stokes, P. Louis, M. A. Jones, and I. R. Booth. 1999. Protection of *Escherichia coli* cells against extreme turgor by activation of MscS and MscL mechanosensitive channels: Identification of genes required for MscS activity. *EMBO J.* 18:1730-1737.
7. Sukharev, S. I., W. J. Sigurdson, C. Kung, and F. Sachs. 1999. Energetic and spatial parameters for gating of the bacterial large conductance mechanosensitive channel, MscL. *J. Gen. Physiol.* 113:525-540.
8. Sukharev, S. I., P. Blount, B. Martinac, F. R. Blattner, and C. Kung. 1994. A large-conductance mechanosensitive channel in *E. coli* encoded by *mscL* alone. *Nature.* 368:265-268.
9. Maurer, J. A., D. E. Elmore, H. A. Lester, and D. A. Dougherty. 2000. Comparing and contrasting *Escherichia coli* and *Mycobacterium tuberculosis* mechanosensitive channels (MscL). New gain of function mutations in the loop region. *J. Biol. Chem.* 275:22238-22244.
10. Anishkin, A., V. Gendel, N. A. Sharifi, C. S. Chiang, L. Shirinian, H. R. Guy, and S. Sukharev. 2003. On the conformation of the COOH-terminal domain of the large mechanosensitive channel MscL. *J. Gen. Physiol.* 121:227-244.
11. Ajouz, B., C. Berrier, A. Garrigues, M. Besnard, and A. Ghazi. 1998. Release of thioredoxin via the mechanosensitive channel MscL during osmotic downshock of *Escherichia coli* cells. *J. Biol. Chem.* 273:26670-26674.

12. Berrier, C., A. Garrigues, G. Richarme, and A. Ghazi. 2000. Elongation factor Tu and DnaK are transferred from the cytoplasm to the periplasm of *Escherichia coli* during osmotic downshock presumably via the mechanosensitive channel mscL. *J. Bacteriol.* 182:248-251.
13. Vazquez-Laslop, N., H. Lee, R. Hu, and A. A. Neyfakh. 2001. Molecular sieve mechanism of selective release of cytoplasmic proteins by osmotically shocked *Escherichia coli*. *J. Bacteriol.* 183:2399-2404.
14. Cruickshank, C. C., R. F. Minchin, A. C. Le Dain, and B. Martinac. 1997. Estimation of the pore size of the large-conductance mechanosensitive ion channel of *Escherichia coli*. *Biophys. J.* 73:1925-1931.
15. Chang, G., R. H. Spencer, A. T. Lee, M. T. Barclay, and D. C. Rees. 1998. Structure of the MscL homolog from *Mycobacterium tuberculosis*: a gated mechanosensitive ion channel. *Science.* 282:2220-2226.
16. Blount, P., S. I. Sukharev, P. C. Moe, M. J. Schroeder, H. R. Guy, and C. Kung. 1996. Membrane topology and multimeric structure of a mechanosensitive channel protein of *Escherichia coli*. *EMBO J.* 15:4798-4805.
17. Blount, P., S. I. Sukharev, M. J. Schroeder, S. K. Nagle, and C. Kung. 1996. Single residue substitutions that change the gating properties of a mechanosensitive channel in *Escherichia coli*. *Proc. Natl. Acad. Sci. USA.* 93:11652-11657.
18. Blount, P., S. I. Sukharev, P. C. Moe, B. Martinac, and C. Kung. 1999. Mechanosensitive channels of bacteria. *Methods Enzymol.* 294:458-482.
19. Sukharev, S. I., B. Martinac, V. Y. Arshavsky, and C. Kung. 1993. Two types of mechanosensitive channels in the *Escherichia coli* cell envelope: Solubilization and functional reconstitution. *Biophys. J.* 65:177-183.
20. Ou, X., P. Blount, R. J. Hoffman, and C. Kung. 1998. One face of a transmembrane helix is crucial in mechanosensitive channel gating. *Proc. Natl. Acad. Sci. USA.* 95:11471-11475.
21. Yoshimura, K., A. Batiza, M. Schroeder, P. Blount, and C. Kung. 1999. Hydrophilicity of a single residue within MscL correlates with increased channel mechanosensitivity. *Biophys. J.* 77:1960-1972.
22. Clayton, D., G. Shapovalov, J. A. Maurer, D. A. Dougherty, H. A. Lester, and G. G. Kochendoerfer. 2004. Total chemical synthesis and electrophysiological characterization of mechanosensitive channels from *Escherichia coli* and *Mycobacterium tuberculosis*. *Proc. Natl. Acad. Sci. USA.* 101:4764-4769.
23. Hallett, F. R., J. Marsh, B. G. Nickel, and J. M. Wood. 1993. Mechanical properties of vesicles. II. A model for osmotic swelling and lysis. *Biophys. J.* 64:435-442.

24. Mui, B. L., P. R. Cullis, E. A. Evans, and T. D. Madden. 1993. Osmotic properties of large unilamellar vesicles prepared by extrusion. *Biophys. J.* 64:443-453.
25. White, G., J. Pencer, B. G. Nickel, J. M. Wood, and F. R. Hallett. 1996. Optical changes in unilamellar vesicles experiencing osmotic stress. *Biophys. J.* 71:2701-2715.
26. Szoka, F., Jr., and D. Papahadjopoulos. 1980. Comparative properties and methods of preparation of lipid vesicles (liposomes). *Annu. Rev. Biophys. Bioeng.* 9:467-508.
27. Paternostre, M. T., M. Roux, and J. L. Rigaud. 1988. Mechanisms of membrane protein insertion into liposomes during reconstitution procedures involving the use of detergents. 1. Solubilization of large unilamellar liposomes (prepared by reverse-phase evaporation) by triton X-100, octyl glucoside, and sodium cholate. *Biochemistry.* 27:2668-2677.
28. Szoka, F., F. Olson, T. Heath, W. Vail, E. Mayhew, and D. Papahadjopoulos. 1980. Preparation of unilamellar liposomes of intermediate size (0.1-0.2 μmol) by a combination of reverse phase evaporation and extrusion through polycarbonate membranes. *Biochim. Biophys. Acta.* 601:559-571.
29. Ertel, A., A. G. Marangoni, J. Marsh, F. R. Hallett, and J. M. Wood. 1993. Mechanical properties of vesicles. I. Coordinated analysis of osmotic swelling and lysis. *Biophys. J.* 64:426-434.
30. Hope, M. J., M. B. Bally, G. Webb, and P. R. Cullis. 1985. Production of large unilamellar vesicles by a rapid extrusion procedure—Characterization of size distribution, trapped volume and ability to maintain a membrane-potential. *Biochim. Biophys. Acta.* 812:55-65.
31. Mayer, L. D., M. J. Hope, and P. R. Cullis. 1986. Vesicles of variable sizes produced by a rapid extrusion procedure. *Biochim. Biophys. Acta.* 858:161-168.
32. Frisken, B. J., C. Asman, and P. J. Patty. 2000. Studies of vesicle extrusion. *Langmuir.* 16:928-933.
33. Hunter, D. G., and B. J. Frisken. 1998. Effect of extrusion pressure and lipid properties on the size and polydispersity of lipid vesicles. *Biophys. J.* 74:2996-3002.
34. Haugland, R. P. 1996. *Handbook of Fluorescent Probes and Research Chemicals, Sixth Edition.* Eugene, OR: Molecular Probes, Inc.
35. Sanny, C. G., and J. A. Price. 1999. Analysis of nonlinear quenching of terbium(III):dipicolinic acid complex fluorescence by chelators and chelate-conjugated macromolecules. *Bioconjug. Chem.* 10:141-145.

36. Rosen, D. L., C. Sharpless, and L. B. McGown. 1997. Bacterial spore detection and determination by use of terbium dipicolinate photoluminescence. *Anal. Chem.* 69:1082-1085.
37. Wilschut, J., N. Duzgunes, R. Fraley, and D. Papahadjopoulos. 1980. Studies on the mechanism of membrane-fusion—Kinetics of calcium-ion induced fusion of phosphatidylserine vesicles followed by a new assay for mixing of aqueous vesicle contents. *Biochemistry.* 19:6011-6021.
38. Aranda, F. J., M. P. Sanchez-Migallon, and J. C. Gomez-Fernandez. 1996. Influence of alpha-tocopherol incorporation on Ca(2+)-induced fusion of phosphatidylserine vesicles. *Arch. Biochem. Biophys.* 333:394-400.
39. Bentz, J., N. Duzgunes, and S. Nir. 1983. Kinetics of divalent-cation induced fusion of phosphatidylserine vesicles—Correlation between fusogenic capacities and binding affinities. *Biochemistry.* 22:3320-3330.
40. Lopezmarin, L. M., D. Quesada, F. Lakhdarghazal, J. F. Tocanne, and G. Laneelle. 1994. Interactions of mycobacterial glycopeptidolipids with membranes—Influence of carbohydrate on induced alterations. *Biochemistry.* 33:7056-7061.
41. Srinivas, S. K., R. V. Srinivas, G. M. Anantharamaiah, J. P. Segrest, and R. W. Compans. 1992. Membrane interactions of synthetic peptides corresponding to amphipathic helical segments of the Human-Immunodeficiency-Virus Type-1 envelope glycoprotein. *J. Biol. Chem.* 267:7121-7127.
42. van Kan, E. J. M., A. van der Bent, R. A. Demel, and B. de Kruijff. 2001. Membrane activity of the peptide antibiotic clavanin and the importance of its glycine residues. *Biochemistry.* 40:6398-6405.
43. Olbrich, K., W. Rawicz, D. Needham, and E. Evans. 2000. Water permeability and mechanical strength of polyunsaturated lipid bilayers. *Biophys. J.* 79:321-327.
44. Silvius, J. R. 1982. *Lipid-Protein Interactions*. New York: John Wiley & Sons, Inc.
45. Furuya, K., and T. Mitsui. 1979. Phase-transitions in bilayer membranes of dioleoyl-phosphatidylcholine-dipalmitoyl-phosphatidylcholine. *J. Phys. Soc. Japan.* 46:611-616.
46. Sukharev, S., S. R. Durell, and H. R. Guy. 2001. Structural models of the MscL gating mechanism. *Biophys. J.* 81:917-936.
47. Needham, D., and R. S. Nunn. 1990. Elastic deformation and failure of lipid bilayer membranes containing cholesterol. *Biophys. J.* 58:997-1009.
48. Kloda, A., and B. Martinac. 2001. Mechanosensitive channel of *Thermoplasma*, the cell wall-less archaea: Cloning and molecular characterization. *Cell Biochem. Biophys.* 34:321-347.

49. Perozo, E., A. Kloda, D. M. Cortes, and B. Martinac. 2002. Physical principles underlying the transduction of bilayer deformation forces during mechanosensitive channel gating. *Nat. Struct. Biol.* 9:696-703.
50. Shapovalov, G., R. Bass, D. C. Rees, and H. A. Lester. 2003. Open-state disulfide crosslinking between *Mycobacterium tuberculosis* mechanosensitive channel subunits. *Biophys. J.* 84:2357-2365.
51. Maurer, J. A., and D. A. Dougherty. 2001. A high-throughput screen for MscL channel activity and mutational phenotyping. *Biochim. Biophys. Acta.* 1514:165-169.